Efficient slow light coupling into photonic crystals

C. Martijn de Sterke, J. Walker,
CUDOS, School of Physics, University of Sydney, NSW 2006, Australia

Kokou B. Dossou and Lindsay C. Botten
CUDOS, Department of Mathematical Sciences, University of Technology, Sydney, NSW 2007, Australia
m.desterke@physics.usyd.edu.au

Abstract: We study light coupling between two photonic crystal waveguides, one of which supports slow light. We show theoretically that a short photonic crystal waveguide between the two that need to be coupled, can lead to a vanishingly small reflectivity. The design relies on the analogy with a $\lambda/4$ anti-reflection layer in thin-film optics. We find that some of the usual relationships between the Fresnel coefficients at an interface no longer hold.

OCIS codes: (230.7370) Waveguides; (130.2790) Guided waves; (050.2230) Fabry-Perot; (250.5300) Photonic integrated circuits; (050.1960) Diffraction theory

References and links

1. Y. A. Vlasov, M. O'Boyle, H. F. Hamann, and S. J. McNab, "Active control of slow light on a chip with photonic crystal waveguides," Nature **438**, 65-69 (2005).
2. R. S. Jacobsen, *et al.*, "Strained silicon as a new electro-optic material," Nature **441**, 199-202 (2006).
3. J. B. Khurgin, "Optical buffers based on slow light in electromagnetically induced transparent media and coupled resonator structures: comparative analysis," J. Opt. Soc. Am. B **22**, 1062-1074 (2005).
4. T. D. Happ, M. Kamp, and A. Forchel, "Photonic crystal tapers for ultracompact mode conversion," Opt. Lett. **26**, 1102-1104 (2001).
5. K. Dossou, L. C. Botten, S. Chen, J. Brnovic, R. C. McPhedran, and C. M. de Sterke, "Efficient couplers for photonic crystal waveguides," Opt. Commun. **265**, 207-219 (2006).
6. P. Pottier, M. Gnan, and R. M. De La Rue, "Efficient coupling into slow-light photonic crystal channel guides using photonic crystal tapers," Opt. Express **15**, 6560-6575 (2007).
7. H. A. Macleod, "Thin Film Optical Filters," 3rd Edition (Institute of Physics Pub., Bristol, 2001), Ch. 3.
8. P. Velha, J. P. Hugonin, and P. Lalanne, "Compact and efficient injection of light into band-edge slow-modes," Opt. Express **15**, 6102-6112 (2007).
9. N. Ozaki, Y. Kitagawa, Y. Takata, N. Ikeda, Y. Watanabe, A. Mizutani, Y. Sugimoto, and K. Asakawa, "High transmission recovery of slow light in a photonic crystal waveguide uing a hetero group velocity waveguide," Opt. Express **13**, 7974-7982 (2007).
10. L. C. Botten, T. P. White, C. M. de Sterke, R. C. McPhedran, A. A. Asatryan, and T. N. Langtry, "Photonic crystal devices modelled as grating stacks," Opt. Express **12**, 1592-1604 (2004).
11. L. C. Botten, T. P. White, A. A. Asatryan, and T. N. Langtry, C. M. de Sterke, R. C. McPhedran, "Bloch mode scattering matrix methods for modelling extended photonic crystal structures. Part 1: Theory," Phys. Rev. E **70**, 056606:1-13 (2004).
12. K. Dossou, M. A. Byrne, and L. C. Botten, "Finite element computation of grating scattering matrices and application to photonic crystal band calculations," J. Comp. Phys. **219**, 120-143 (2006).
13. L. C. Botten, T. P. White, A. A. Asatryan, T. N. Langtry, C. M. de Sterke and R. C. McPhedran, "Photonic crystal devices modelled as grating stacks: matrix generalizations of thin film optics," Opt. Express **12**, 1592–1604 (2004).

#84750 - $15.00 USD Received 3 Jul 2007; revised 10 Aug 2007; accepted 14 Aug 2007; published 16 Aug 2007

1. Introduction

One of the emerging applications of photonic crystals (PCs) is their capacity to generate slow light modes. This arises because of the unprecedented ability to manipulate the dispersion relation of light in PCs. Slow light itself has a number of important applications, such as increased field amplitude, thereby increasing the strength of nonlinear interactions, and reduced fringe spacing in interferometers, and hence increasing their sensitivity, for example, when used as a modulator [1, 2]. Longer term applications include all-optical delay lines and buffers [3].

One of the factors limiting the use of slow light in PCs is the difficulty of coupling the light into and out of the structure, essentially because of a large impedance mismatch between the slow light region and the other waveguides that do not support slow light. One way of overcoming an impedance mismatch is by using a taper [4, 5, 6]. Though this works well for most wavelengths in a PC bandgap, and indeed efficient broadband tapers have been designed, the taper would need to be very long in order to deal with slow modes. The reason is that the taper needs to be long in comparison with the effective wavelength of the light. In slow light regions, however, which occur usually near the Brillouin zone center or edge, the taper length diverges as the group velocity $v_g \to 0$. It is true that a 96% efficient coupler into a slow mode using a taper with a length of only eight lattice constants was designed by Pottier *et al.* [6]. In this case, however, the most efficient coupling was achieved using residual Fabry-Perot effects. In contrast, in the work reported here, these effects are our primary interest and, in fact, we demonstrate that perfect coupling using Fabry-Perot effects can be achieved.

In optics, the challenge of reducing reflection at an impedance mismatch is a very old one. Apart from tapering, the other method by which to reduce reflection is the use of a stack of thin matching layers, the best known example of which is the application of a thin-film stack to reduce the reflection when light is incident on glass from air. The simplest and thinnest of these coatings is a single layer of thickness $\lambda/4$ and refractive index $n_2 = \sqrt{n_1 n_3}$, where n_1 and n_3 are the refractive indices of the semi-infinite media that are to be matched. This layer corresponds to a resonance of a balanced Fabry-Perot cavity, and thus provides perfect transmission, even if only at a single wavelength of interest. More complicated coatings, consisting of multiple layers, have been designed to reduce reflection over wide wavelength ranges [7].

Here, we describe a method for efficient light coupling into a slow-light waveguide by using a generalization of the $\lambda/4$ layer, thereby guaranteeing perfect matching at a single wavelength. It is somewhat similar to that of Velha *et al.*, although their approach depends on the details of the Bloch functions [8]. A heterostructure approach was also implemented by Ozaki *et al.* to improve the coupling efficiency [9]. We work with a two-dimensional geometry [6] in order to avoid the considerable computational demands for three-dimensional simulations, and because the design strategy is identical in the two cases. We discuss this further in Section 4.

2. Geometry and theoretical background

In order to design an anti-reflection coating for a PC, we must map the PC properties onto those of thin-film stacks. Since we have done so in previous work [10, 11], here we give only the essential results that make this analogy clear. We consider the generic geometry of Fig. 1(a) consisting of two semi-infinite hole-type PCs, labeled by 1 and 3, each with a PC waveguide that differs from one other. The PCs have lattice constant d, background refractive index $n = 3.4$, and normalized hole radius $a/d = 0.23$, with the electric field orthogonal to the axes of the holes ($H_{//}$ polarization). The bulk PC has a bandgap for the frequencies $0.201 < d/\lambda < 0.227$.

The waveguide in PC 3 has a width of $w_3 = 0.9\sqrt{3}d$, so that for frequencies just above its cut-off at $d/\lambda = 0.211918$ it supports a slow mode; at the frequency $d/\lambda = 0.211987$ that we consider here, for instance, the group velocity is $v_g = 0.01\ c$. In contrast, in PC 1 the waveguide

#84750 - $15.00 USD Received 3 Jul 2007; revised 10 Aug 2007; accepted 14 Aug 2007; published 16 Aug 2007

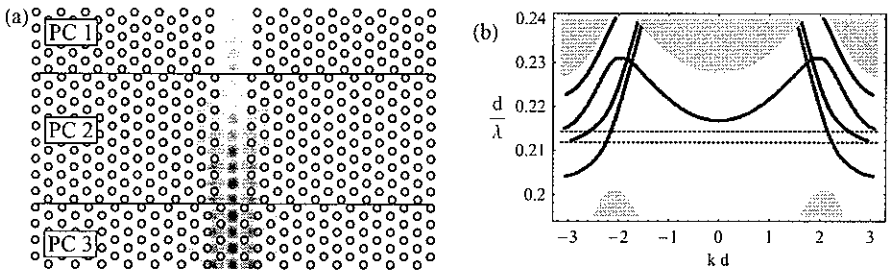

Fig. 1. (a) (1.14 MB) Schematic of the geometry and field animation for the perfectly matched structure: light from above in the fundamental mode of PC 1 ($v_g = 0.157\ c$) is incident on the lower semi-infinite PC 3 ($v_g = 0.01\ c$). The transmission is perfect thanks to the inclusion of an appropriately chosen PC 2 which acts as an anti-reflection coating. (b) Associated band structure for PC 1 (red) and PC 3 (blue); both waveguides have single mode operation for $0.211918 \leq d/\lambda \leq 0.214481$ indicated by the horizontal dashed lines.

has a width $w_1 = \sqrt{3}d$ leading to $v_g = 0.157\ c$ at the same frequency. If these two waveguides were to be butt-coupled, the transmission would be approximately 41%. The band structures for PC 1 and PC 3, shown in Fig. 1(b), are essentially similar, apart for the dispersion of waveguide modes. We model each row of cylinders as a supercell of period D. Note that when the waveguides have different widths, we need to adjust the cylinder spacing so that each segment has a common supercell period. To maintain the integrity of the bandgap we maintain the spacing of the two cylinders adjacent to each side of the guide wall at $d_x = \sqrt{3}d$. The remaining cylinders are then equally spaced to fit in to the remainder of the supercell, with a spacing of which differs slightly from d_x [5]. Though here the waveguides that we consider have different widths, they could also differ in the size of the holes immediately surrounding the guide.

Within each uniform part of the structure, (*i.e.*, within each section PC 1, PC 2, and PC 3) the field propagates as a superposition of Bloch functions, each with Bloch factor $\mu = \exp(ikd)$, where k is the component of the Bloch vector in the propagation direction; k is real for propagating states and is complex otherwise. The connection of the field between two uniform structures is described by Fresnel reflection and transmission scattering matrices $\mathbf{R}_{ij}$ and $\mathbf{T}_{ij}$, respectively, for propagation in the direction from medium i to medium j. The pq element of these matrices denotes the amplitude reflection or transmission coefficient from Bloch function q into Bloch function p at the interface. While the elements of the scattering matrices can be computed using a variety of approaches, here we use the finite element based transfer matrix method [12].

We showed earlier [11, 13] that, for structures consisting of three piecewise-uniform PCs such as in Fig. 1(a), the reflection matrix can be expressed as

$$\mathbf{R} = \mathbf{R}_{12} + \mathbf{T}_{21}\mathbf{\Lambda}_2{}^m\mathbf{R}_{23}\mathbf{\Lambda}_2{}^m\left(\mathbf{I} - \mathbf{R}_{21}\mathbf{\Lambda}_2{}^m\mathbf{R}_{23}\mathbf{\Lambda}_2{}^m\right)^{-1}\mathbf{T}_{12}, \tag{1}$$

where m is the number of layers in PC 2 and $\mathbf{\Lambda}_2 = \text{diag}\ \{\mu_j\}$ is a diagonal matrix of Bloch factors. As mentioned previously, the structure in Fig. 1(a) supports a single mode in each propagation direction, while the remaining modes are evanescent. In particular, in PC 2, we have $|\mu_1| = 1$, with all other $|\mu_j| < 1$ ($j \geq 2$). For m sufficiently large, $\mathbf{\Lambda}^m \approx \mu_1^m \boldsymbol{u}\boldsymbol{u}^T$ where $\boldsymbol{u} = [1, 0, 0, \ldots]^T$, thus effectively eliminating any evanescent coupling between the lower and upper interfaces of PC 2 [11, 13]. In practice, this is an excellent approximation, with negligible differences even for couplers of as few as $m = 3$ layers, and with the approximation improving exponentially with increasing m. This allows us to truncate the full set of modes in Eq. (1) to

#84750 - $15.00 USD Received 3 Jul 2007; revised 10 Aug 2007; accepted 14 Aug 2007; published 16 Aug 2007

just the single propagating modes, in turn allowing us to replace all matrices by scalars.

In this way, the PC problem is reduced to one that is equivalent to that of a thin-film stack. There are, however, some subtleties in the argument that need to be worked through. We now replace all matrices (written in uppercase bold typeface) in Eq. (1) by scalar elements (normal type face): for Fresnel coefficients, for example, $r_{12} \equiv (\boldsymbol{R}_{12})_{11}$ denotes the sole ((1 1) subscript) propagating mode element, with equivalent forms for the other Fresnel coefficients; while for the Bloch factors, we replace $\boldsymbol{\Lambda}_2^m$ by μ^m, in which μ is shorthand for μ_1—the sole propagating Bloch factor in PC 2. Thus, Eq. (1) reduces to

$$r = \frac{r_{12} + f_{12} r_{23} \mu^{2m}}{1 - r_{21} r_{23} \mu^{2n}}, \quad \text{where} \quad f_{12} = t_{12} t_{21} - r_{12} r_{21}, \tag{2}$$

which is identical to the standard Airy formula, with the exception of the factor f_{12}. This factor f_{12} also appears in the corresponding derivation for thin films, but its value there is $f_{12} = 1$. While the assumption that $f_{12} = 1$ is valid also in 1D PC systems, this cannot be taken for granted in more complex 2D and 3D PCs due to the multiplicity of modes (propagating and evanescent) and the complex interrelationships between them, expressed by the elements of the Fresnel matrices. For a general 2D system, it is straightforward to show [13] that for the full (untruncated) Fresnel matrices, $\boldsymbol{T}_{12}\boldsymbol{T}_{21} = \boldsymbol{I} - \boldsymbol{R}_{21}^2$, the form of which leads one to suggest that $f_{12} = 1$. Even though this general matrix form is comparable with the scalar form (f_{12}), there is no simple relationship between $\mathbf{R}_{12}$ and $\mathbf{R}_{21}$ and so the scalar property does not follow from the matrix property. Instead, we must begin with the S-matrix of the truncated system,

$$\boldsymbol{S} = \begin{pmatrix} r_{12} & t_{21} \\ t_{12} & r_{21} \end{pmatrix}, \tag{3}$$

which, for lossless structures, we know to be unitary [11], *i.e.*, $\boldsymbol{S}\boldsymbol{S}^H = \boldsymbol{S}^H\boldsymbol{S} = \boldsymbol{I}$. Accordingly, its determinant, $\det \boldsymbol{S} = -f_{12}$, has unit magnitude and so we may write $f_{12} = e^{2i\phi_{12}}$. From the unitarity of $\boldsymbol{S}$, we may derive the explicit relation, $t_{21}/t_{12}^* = -r_{21}/r_{12}^* \equiv g_{12}$, where $|g_{12}| = 1$ since, by reciprocity, $t_{12} = t_{21}$. Some simple manipulation then reveals that $f_{12} = g_{12}\left(|t_{12}|^2 + |r_{12}|^2\right) = g_{12}$ (by energy conservation), from which it follows that $\phi_{12} = \arg t_{12} = \arg t_{21}$. This, in turn, leads us to consider scaled Fresnel coefficients—$\tilde{r}_{12} = r_{12}e^{-i\phi_{12}}$, $\tilde{r}_{21} = r_{21}e^{-i\phi_{12}}$, together with identical forms for $\tilde{t}_{12}$ and $\tilde{t}_{21}$, thus leading to $\tilde{f}_{12} \equiv \tilde{t}_{12}\tilde{t}_{21} - \tilde{r}_{12}\tilde{r}_{21} = 1$. Under this scaling, $\tilde{t}_{12} = \tilde{t}_{21}$ are real numbers, while the reflection coefficients are, in general complex, satisfying $\tilde{r}_{21} = -\tilde{r}_{12}^*$ — a generalization of the familiar relation $r_{21} = -r_{12}$ applicable in 1D systems.

We now consider the interpretation of the scaled forms, beginning with $\tilde{r}_{12}$. It is easy to show that this is the reflection coefficient r_{12} translated by the phase $\phi_{12}/2$ below the original phase origin O_{12} at the PC 1–PC 2 interface. We are thus led to introduce new phase origin planes at A_{12} and B_{12}, respectively $\phi_{12}/2$ (in phase) above and below O_{12} (see Fig. 2(a)). With these definitions, $\tilde{r}_{12}$ has its input and output origins at B_{12}, while $\tilde{r}_{21}$ has input and output origins at A_{12}. The transmission coefficients differ in that their input and output phase origins occur on different planes: $\tilde{t}_{12}$ has input and output origins at B_{12} and A_{12} respectively, while $\tilde{t}_{21}$ has the corresponding origins of A_{12} and B_{12}. The same applies at the PC 2–PC 3 interface, but with phase shift ϕ_{23}, new phase origins A_{23} and B_{23}, and scaled Fresnel coefficients $\tilde{r}_{23}$, $\tilde{r}_{32}$ etc.

With this, we may recast Eq. (2) in precisely the Airy form. For completeness, we present expressions for both r and t

$$r = e^{i\phi_{12}} \frac{\tilde{r}_{12} + \tilde{r}_{23}e^{2i\psi}}{1 - \tilde{r}_{21}\tilde{r}_{23}e^{2i\psi}}, \qquad t = e^{i(\phi_{12}+\phi_{23})/2} \frac{\tilde{t}_{12}\tilde{t}_{23}e^{i\psi}}{1 - \tilde{r}_{21}\tilde{r}_{23}e^{2i\psi}}. \tag{4}$$

with $\psi = mkd + (\phi_{12} + \phi_{23})/2$, where the arguments of the Fresnel coefficients shift the resonances in the usual way (*c.f.* Fig. 2(a)) and the leading term $e^{i\phi_{12}}$ denotes the translation of the input and output phase origin to O_{12} from B_{12}.

#84750 - $15.00 USD Received 3 Jul 2007; revised 10 Aug 2007; accepted 14 Aug 2007; published 16 Aug 2007

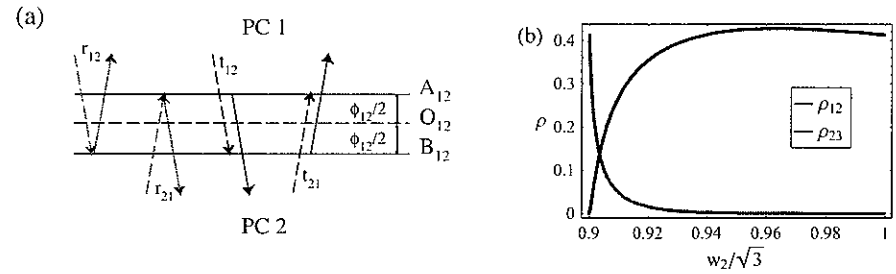

Fig. 2. (a) Illustration of the interpretation of ϕ_{12} through the use of alternative phase origins. (b) Interface reflectances ρ_{21} and ρ_{23} versus the width w_2 of the waveguide in PC2.

3. Design of the coupling region

As mentioned in Section 2, we operate at the frequency $d/\lambda = 0.211987$, close to the cutoff of the mode in PC 3, where $v_g = 0.01\ c$. At this frequency, $v_g \approx 0.157\ c$ in PC 1. To design an appropriate PC 2, recall that a Fabry-Perot interferometer exhibits perfect transmission provided two requirements are satisfied: (i) the reflectance of both mirrors must be the same, and (ii) the phase upon a full round trip through the cavity must be a multiple of 2π. We first consider Issue (i), which requires us to choose PC 2 so that

$$\rho_{21} = \rho_{23}, \tag{5}$$

where $\rho_{ij} = |r_{ij}|^2$ is an interface reflectance. The phases of the amplitude reflection coefficients contribute to the length of PC 2, as discussed in Section 2. Now if $w_2 = w_1$, $\rho_{21} = 0$, and $\rho_{23} \neq 0$. If w_2 decreases, then ρ_{21} increases, while ρ_{23} decreases until $\rho_{23} = 0$ when $w_2 = w_3$. Therefore, at some value $w_1 < w_2 < w_3$, we expect Eq. (5) to be satisfied, as confirmed in Fig. 2(b): we find that $\rho_{21} = \rho_{23} \approx 0.137$ at $w_2 = 0.90356\ \sqrt{3}d$.

Having found the value for w_2 required for perfect coupling, we now consider Issue (ii), the length m. In a balanced Fabry-Perot cavity the reflectance varies between $\rho = 0$ and $\rho = |r|^2 = 4\rho_{12}/(1+\rho_{12})^2 \approx 0.42$ (where $\rho = |r|^2$), depending on the cavity's length. The former (latter) respectively occur at resonances (antiresonances). This is illustrated in Fig. 3(a), which shows the structure's reflectance versus coupler length m. The reflectance has the shape expected for a Fabry-Perot-like structure. The reflectance is very low for $m = 8, 23, 38, \ldots$, with the period of 15 layers being consistent with $kd = 2.93189 \approx 14\pi/15$ in PC 2.

The reflectance of the complete structure with $m = 8$ layers is given in Fig. 3(b). At the design wavelength, where $v_g = 0.01c$ in PC 3, the reflectance is as low as $\rho \approx 0.0023$, a reduction of more than a factor of 100 in comparison with that achievable by butt-coupling PC 1 and PC 3. The field animation associated with Fig. 1(a) shows the almost reflectionless propagation of the fundamental mode in PC 1, through the coupler, into the slow light waveguide. The residual reflectance is associated with the fact that m can take only integer values. Of course this residual reflectance can be eliminated if the design wavelength is allowed to vary slightly, but this would require a slight adjustment of the width of the waveguide in PC 2 as well. Nonetheless, Fig. 3(b) shows that for our parameters the minimum reflectance occurs closer to $v_g = 0.0093\ c$ where $\rho = 0.0015$. For our design, the bandwidth of the low-reflectance region is limited by the fact that the mode in PC 3 is close to cutoff, so that its group velocity varies rapidly with frequency.

#84750 - $15.00 USD Received 3 Jul 2007; revised 10 Aug 2007; accepted 14 Aug 2007; published 16 Aug 2007

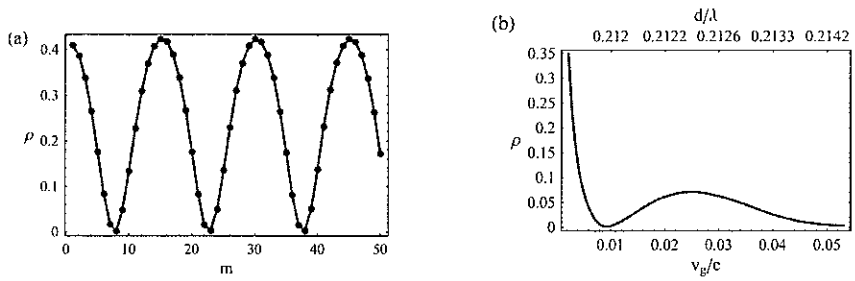

Fig. 3. (a) Reflectance ρ of the entire structure versus m, the length of PC 2, for a waveguide width $0.90356\sqrt{3}d$. (b) Reflectance versus group velocity (bottom scale) in PC 3 and normalized frequency (top scale) for $w_2 = 0.90356\sqrt{3}d$ and $m = 8$.

4. Discussion and Conclusion

We have seen that the design of the anti-reflection layer is very similar to that for a thin-film stack. One interesting difference is that in thin-film design the layer thickness can be arbitrary, but that the refractive index of the layer can take only the discrete values associated with the available materials. In contrast, here the length is discretized by the need to have an integer number of periods in PC 2, while the equivalent of the refractive index can be chosen arbitrarily since, for example, the waveguide width can be varied continuously. It is expected that the discreteness of the available values for m becomes less important in more complicated, anti-reflection structures, which, however, are also longer.

As mentioned in Section 1 the treatment here has been two-dimensional. Although the structure was designed so that each of the waveguides operate below the light line, whereby the out-of-plane losses associated with propagation are eliminated, resonant reflection does lead to such losses. Since the finesse of the device is not high, the out-of-plane losses are likely to be modest, although this is the subject of a future study. The modest finesse also ensures that phase variations of the transmission have negligible effect on the transmission of pulses. Another issue that needs to be resolved is the accuracy with which the PCs need to be fabricated; though theoretically the best results are obtained for $w_2 = 0.90356\sqrt{3}d$, such accuracy probably cannot be achieved in practice, and so the effect of fabrication tolerances also needs to be investigated.

One of the issues that needed to be addressed in the analysis was the nature of the relationships between various Fresnel reflection and transmission coefficients. While one might expect that the very strict relationships for the interfaces between uniform media no longer hold when considering PCs, it is striking that the relationships generalize to depend only on single parameters, ϕ_{12} and ϕ_{23}, that are associated with the "extended" nature of the matching interfaces.

In conclusion, we have shown that the in-plane reflection losses between two PC waveguides that support modes with widely different group velocities can be reduced to arbitrarily low values, limited only by the fact that the length of the intermediate waveguide needs to be an integer number of periods. Though this result is interesting and useful in its own right, more generally it opens the way for more sophisticated "multilayer" designs, which can cover a wider band of wavelengths, and the performance of which is less limited by the discreteness of the available parameters. The design approach is very general and should be applicable to a variety of PC coupling problems such as the coupling between a PC waveguide and free space.

#84750 - $15.00 USD Received 3 Jul 2007; revised 10 Aug 2007; accepted 14 Aug 2007; published 16 Aug 2007

Acknowledgments

The support of the Australian Research Council through its Centres of Excellence and Discovery Grants programs is acknowledged.

#84750 - $15.00 USD Received 3 Jul 2007; revised 10 Aug 2007; accepted 14 Aug 2007; published 16 Aug 2007